Accelerated Weathering of Recycled Polypropylene Packaging Bag Composites Reinforced with Wheat Straw Fibers

Min Yu Chunxia He Runzhou Huang
Junjun Liu Derong Lu

Abstract

In this study, there were two kinds of recycled polypropylene (RPP) packaging bags, RPP disposable packaging bags (RPP-DB) and RPP woven bags (RPP-WB), used as matrix reinforced with wheat straw fiber (WSF). The aim of this study was to investigate the relative degradation behavior of WSF/RPP composites with two RPP matrices under weathering conditions. The RPP packaging bags were blended with WSF by a two-roll mill mixer and then molded by a compression molding machine. The effects of accelerated weathering on the surface morphology, surface color, surface chemistry, thermal properties, and mechanical properties were evaluated after distinct periods; the total time of exposure of the composites in a QUV-accelerated weathering tester was 1,200 hours. The weathering degradation process of WS/RPP-DB was gradual from surface to interior, whereas the internal collapse aggravated the performance reduction of WS/RPP-WB. The weathering resulted in significant discoloration. The photobleaching of WS/RPP-DB was faster than of WS/RPP-WB. The Fourier-transform infrared spectrum suggested that the color change was closely related to the formation of carbonyl groups and degradation of lignin. After weathering, the thermal properties of WS/RPP-DB and WS/RPP-WB were both decreased. The flexural strength and modulus of WS/RPP strongly decreased with exposure time and was related to the surface crack of composites. The utilization of RPP packaging bags as matrix could be a good candidate of wood–plastic composites for applications in the future.

Wood–plastic composites (WPCs) made from a blend of thermoplastic and lignocellulose fibers are gaining popularity worldwide because of good mechanical properties, low density, low cost, recyclability, and ecofriendliness (Achilias et al. 2008). To address the raw material shortage issues in the plastics industry, researchers in collaboration with WPC enterprises are currently working to develop a substitute for virgin plastic and wood material. However, the performance and appearance of recycled plastic decreases considerably after use, but this can apparently be overcome by regenerating the plastic with a deep color (Kazemi Najafi 2013). To ensure good quality, the share of recycled plastic is restricted to 20 to 30 percent, which greatly limits the application of recycled plastics (Winandy et al. 2004). Therefore, the recycled plastic matrix for WPCs is supposed to have good performance, light color, and be easy to recycle. The polypropylene (PP) packaging bags, such as food bags, cigarette packaging, clothing bags, fertilizer bags, etc., are one of the biggest consumers of PP resin. The average service life of plastic packaging bags is 1 to 2 years in general but practically they are only used once and discarded, which considerably increases the plastic share in municipal solid waste (Meran et al. 2008). Because of the short use time of PP disposable packaging bags, the degradation is less, which can maximize the performance of PP. Meanwhile, many PP disposable packaging bags are transparent, so they contain less ink and are easy to clean and deink. PP woven bags are the other kind of PP

The authors are, respectively, Instructor, College of Mechanical & Electrical Engineering, Shanxi Univ. of Sci. & Technol., Xi'an, China (minyu003@hotmail.com); PhD Professor, College of Engineering, Nanjing Agric. Univ., Nanjing, Jiangsu, China (chunxiahe@hotmail.com [corresponding author]); Associate Professor, College of Material Sci. and Engineering, Nanjing Forestry Univ., Nanjing, China (runzhouhuang@gmail.com); Associate Professor, Changshu Inst. of Technol., Changshu, Jiangsu, China (walhfg96@aliyun.com); and Instructor, Nantong Inst. of Technol., Nantong, Jiangsu, China (derong2000@163.com). This paper was received for publication in December 2014. Article no. 14-00107.

Forest Prod. J. 66(7/8):485–494.
doi:10.13073/FPJ-D-14-00107

packaging bag, and they are widely used in bulk products (Hawkins 2001, Hopewell et al. 2009). It was reported that the tonnage of plastic pollution caused by waste PP woven bags was higher than that of polyethylene packaging in China, which was generally believed to be the major source of plastic pollution (Xing 2009, He 2010). Each PP woven bag is about 80 to 120 g, contains less ink, and can be separated easily from products, resulting in better recycle potential. Therefore, using recycled PP (RPP) disposable packaging bags (RPP-DB) and RPP woven bags (RPP-WB) as WPC matrices has certain advantages on performance, color, and recyclability.

Wheat straw fiber (WSF) can be considered as important potential reinforcing filler for thermoplastic composite because of its excellent mechanical properties and biodegradable and renewable features. China is a large agricultural country that produces thousands of tons of wheat, with an approximate wheat-to-straw ratio of 1.0; an equivalent amount of wheat straw (WS) is produced every year (Lujia et al. 2002). It was reported that nearly 120 million tons of straw have been burned directly, resulting in emission to the atmosphere of 2 million tons of PM2.5 and 100 million tons of carbon dioxide. In addition, it will produce many polycyclic aromatic hydrocarbons, which can increase the risk of cancer and deformity (Zhang et al. 2008, Lin et al. 2010). The utilization of WS as a reinforcement in polymer composites can decrease environmental impacts as well as increase value of the waste material. Therefore, the development of WS/recycled plastic composite materials has important economic and social benefits.

The major issue in WPC outdoor application is its poor weathering properties, as ultraviolet (UV) radiation and moisture are the main elements that cause the change in morphology and chemical, physical, and mechanical properties of WPCs (Matuana et al. 2011, Azwa et al. 2013). For example, the UV degradation mechanisms of PP can be divided into three steps: initiation, propagation, and termination, which are briefly described in Figure 1 (Abdel-Bary 2003). The rate of degradation is high near the surface as O_2 is used up before it can diffuse to the interior (Joseph et al. 2002, Matuana et al. 2011). The UV radiation absorbed by PP modifies the chemical structure, crystallization, and melting behaviors and combines with molecular chain scission. The shorter polymer chains will initiate and propagate cracks on the surface, which leads to light diffusion and deterioration of mechanical properties (Mukhopadhyay and Srikanta 2008). For lignocellulose fibers, degradation occurs because of UV radiation absorption by lignin, formation of quinoid structures, Norrish reactions, and reactions of photoyellowing, which make a significant contribution to discoloration (Beg and Pickering 2008, Butylina et al. 2012a). Moisture can also accelerate degradation and mechanical property loss in WPCs by causing the wood fibers to swell and by inducing cracks in the plastic matrix (Hu et al. 2010).

Although the effects of weathering on wood fiber–reinforced PP have been widely examined, little information is available on WSF-reinforced RPP composites from packaging bags. The aim of this study was to investigate the relative degradation behavior of WSF/RPP composites with two RPP matrices under weathering conditions.

Initiation

$$RH + O_2 \rightarrow R^{\bullet} + HOO^{\bullet} \quad (1)$$

Propagation

$$R^{\bullet} + O_2 \rightarrow ROO^{\bullet}$$
$$ROO^{\bullet} + RH \rightarrow R^{\bullet} + ROOH \quad (2)$$
$$R^{\bullet} + R'H \rightarrow RH + R'^{\bullet}$$

Termination

$$R^{\bullet} + R'^{\bullet} \rightarrow R - R' \quad (3)$$
$$RO^{\bullet} + {}^{\bullet}R \rightarrow ROR$$
$$2ROO^{\bullet} \rightarrow ROOR + O_2$$
$$2RO^{\bullet} \rightarrow ROOR$$

Figure 1.—Ultraviolet degradation mechanisms of polypropylene.

Experimental

Materials

The materials used in this study were WSF and two types of RPP packaging bags, i.e., RPP-DB and RPP-WB. The RPP packaging bags were obtained from Jiulong Regenerated Resources Recycling Co. Ltd, Jiangsu, China. WS came from Youfang Town, Jiangsu Province, China, and was prepared by grinding and screening, using a LH-08B Speed Grinder (Xinchang Hongli, CNC Instruments Inc., Jiangsu, China) with a 60-mesh screen. Silane coupling agent (KH550) from the Yaohua Co. (Shanghai, China) was used to treat WSF. The formulation of the WS/RPP composite was 50 percent WSF and 50 percent RPP. A 50 percent WSF composite formulation was chosen because it was representative of commercially available lumber products.

Sample preparation

WSFs were first ovendried at 105°C for 6 hours to reduce moisture content level to less than 2 percent. A speed mixer (K600-3205, Braun Electric, Germany) was used to mix WSF thoroughly, while stirring an aqueous solution (ethanol:water = 9:1 by weight) including a silane coupling agent (2%, by weight, of WSF) that was sprayed into them at 25°C for 30 minutes. After that, the mixture of WSF was dried at 105°C for 12 hours. The WS/RPP composites were prepared by blending the WSF and PP at 175°C for 5 to 7 minutes on a two-roll mill mixer (X-160 Banbury, Chuangcheng Rubber and Plastic Machinery Co., Ltd., Wuxi, China), after which the melting mixture was laid on a compression molding machine (XLB-0 Vulcanizing Mechine, Shunli Rubber Machinery Co., Ltd., Huzhou, China) at 180°C and 12.5 MPa for 12 minutes. The prepared board dimension was 120 by 100 by 5 mm, and then cut into the required size. All specimens were then conditioned for 72

hours at a temperature of 23°C ± 2°C and a relative humidity of 50 ± 5 percent for later characterization.

Accelerated weathering testing

The samples were subjected to an artificial weathering by exposing to 340-nm fluorescent UV lamps in a QUV accelerated weathering tester (ZN-P Aging Chamber, Nuoweier Electronic Technology Co., Ltd, Suzhou, China) for different intervals of 240, 480, 720, 960, and 1,200 hours. The weathering cycle involved a continuous UV light irradiation of 8 hours (60°C) followed by a water condensation for 4 hours (50°C). The specimens were exposed to the artificial weathering only on one side for all times.

Characterization

Morphology analysis.—The morphologies of selected composite samples were analyzed by a Hitachi S-3600N VP scanning electron microscope (Hitachi Ltd., Tokyo, Japan). The fractured surfaces of selected test samples were coated with platinum to improve the surface conductivity before observation and the samples were observed at an acceleration voltage of 15 kV.

Colorimetric analysis.—The surface color of composites was measured by a chroma meter (Hanpu HP-200, China) according to the CIE L*a*b* color system. Four specimens were taken for each formulation and measured. For each specimens five different points were measured, and the average values were calculated automatically by the chroma meter. The color difference (ΔE) was determined with the procedure outlined in ASTM D2244-15a (ASTM International 2015):

$$\Delta E = (\Delta L^{*2} + \Delta a^{*2} + \Delta b^{2})^{1/2} \quad (1)$$

where ΔL^*, Δa^*, and Δb^* are the total changes on L^*, a^*, and b^* values during weathering, respectively. An increase in L^* means the sample is lightening (i.e., a positive ΔL^* for lightening and a negative ΔL^* for darkening). A positive Δa^* signifies a color shift toward red, and a negative Δa^* signifies a color shift toward green. A positive Δb^* signifies a shift toward yellow, and a negative Δb^* signifies a shift toward blue.

Mechanical properties.—Flexural testing was done with specimens 100 by 10 by 5 mm in a three-point bending mode using a CMT6104 SANS mechanical testing machine (Tesla Industrial systems Co., Guangdong, China) following the GB/T 9341 standard (Standardization Administration of the People's Republic of China [SAC] 2008a). A crosshead speed of 5 mm/min and a span length of 80 mm were used for all tests. Unnotched impact strength was determined from specimens 80 by 10 by 5 mm in size using a XJJ-5 impact tester (Jinjian Testing Instrument Co., Chengde, China) according to the GB/T 1043 standard (SAC 2008b). Five specimens were taken for each test, and average data along with corresponding standard deviation were reported.

FTIR spectra measurement.—The surface chemical changes in composites during accelerated weathering were monitored by a Fourier transform infrared (FTIR) spectrometer (Nicolet iS 10 FT-IR, Thermo Fisher Scientific, USA). The FTIR spectra were obtained in the range 4,000 to 400 cm^{-1} at a resolution of 4 cm^{-1} and a minimum of 60 scans. A typical approach consists of the monitoring of one or more bands of interest in relation to a band that did not change during the weathering process. Because the peak at 2,920 cm^{-1}, which corresponds to asymmetric stretching vibrations of methylene (–CH2–) groups of PP, showed the least change during degradation, it was used as a reference (Zhang et al. 1997, Achilias et al. 2008). The carbonyl index was calculated using the following equation:

$$\text{Carbonyl index} = I_{(1,717)}/I_{(2,920)} \quad (2)$$

where I denotes the intensity. The peak intensity in the carbonyl region normalized using the intensity of peak at 2,920 cm^{-1}, which corresponds to asymmetric stretching vibrations of methylene groups. The lignin index was calculated using the following equation:

$$\text{Lignin index} = I_{(1,508)}/I_{(2,920)} \quad (3)$$

The peak intensity of aromatic skeletal vibration originating from lignin (1,508 cm^{-1}) normalized using the intensity of peak at 2,920 cm^{-1}, which corresponds to asymmetric stretching vibrations of methylene groups (Achilias et al. 2008).

Thermogravimetric analysis.—Thermogravimetric analysis (TGA) was conducted using a STA 449 F3 analyzer (Netzsch, Germany) to study thermal decomposition of the composites. Samples of about 10 mg were heated from 30°C to 700°C at a rate of 10°C/min in an Ar atmosphere. The weight-loss rate was obtained from derivative thermogravimetric data. The onset decomposition temperature (T_{onset}) was defined as the intersection temperature of tangents drawn from the TG curves.

Results and Discussion

Surface morphology

Surface morphology of composites during weathering is shown in Figure 2. Before exposure, the WS/RPP-DB and WS/RPP-WB composites showed a smooth and flat surface, exhibiting that WSF could be completely wrapped by PP matrix (Figs. 2a and 2e). After 240 hours of exposure (Fig. 2b), the bond between WSF and PP was destroyed at first, with cracks around the WSF edge extending and expanding to all around, leaving distinguishable unprotected WSF on the exposed surface. These cracks were considered to be related to the photo-oxidation of PP, which caused chain scission and molecular weight reduction, and would initiate and propagate cracks (Fabiyi et al. 2009). The composites produced from WSF swelled greatly when exposed to water during the condensation process because of its higher hygroscopicity than PP (Reddy et al. 2010). During 240 to 720 hours of exposure, the bared WSF became the main target of UV radiation and water, which made WSF swell when exposed to alternate wetting and drying cycles, and combined with PP bearing alternate stress, resulted in cracks accumulating. Because the swelling WSF created microcracks in the matrix and degraded WSF particles were washed away by condensation water, many smaller cracks were observed (Fig. 2c). Though long-time exposure (1,200 h) caused visible changes on the surface layer, including protrusion and debonding of WSF, WS/RPP-DB still showed a relatively flat surface (Fig. 3a), indicating that the degradation mainly happened on the surface and the overall composites largely remained integral and dense. So for WS/RPP-DB, the weathering degradation process was gradual from surface to interior.

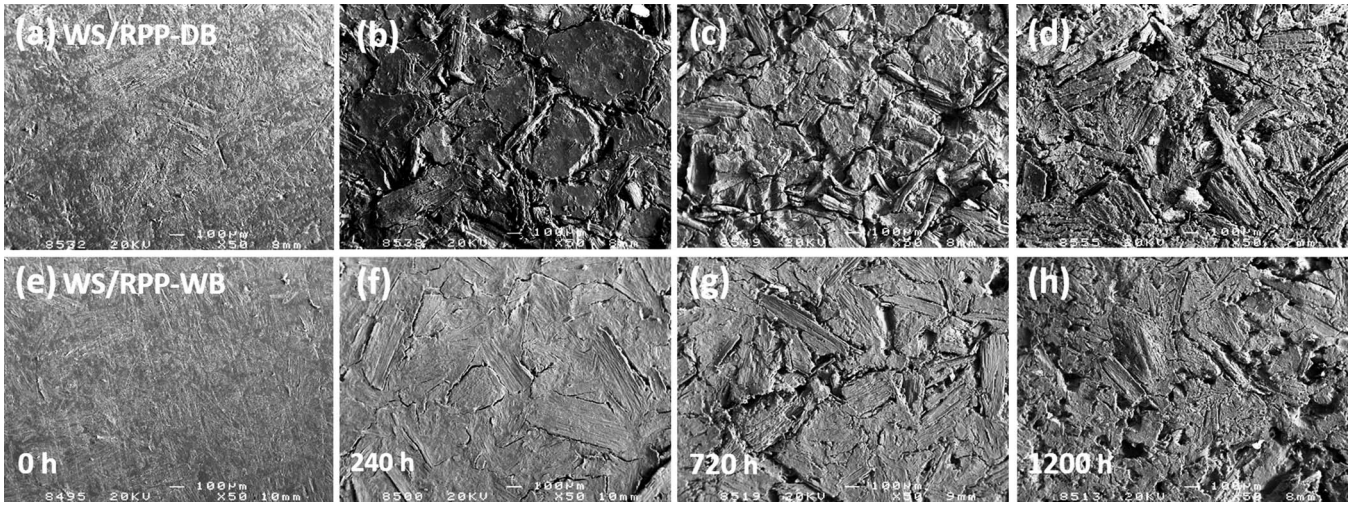

Figure 2.—Scanning electron microscope images of surface of wheat straw (WS)/recycled polypropylene (RPP)–disposable packaging bags (a through d) and WS/RPP–woven bags (e through h) as a function of weathering time.

Figures 2e through 2h present micrographs of weathered surfaces of WS/RPP-WB. After 240 hours of weathering, some tiny cracks and microparticles were observed on the surface of WS/RPP-WB (Fig. 2f). With increasing exposure time, these cracks and microparticles also increased. After 720 hours of exposure, the degraded RPP-WB was unable to bond WSF and formed many deep holes on the surface (Fig. 2g), facilitating UV light and water penetration deeper into deeper composite and further degradation (Stark and Matuana 2006). When the weathering test was carried out to 1,200 hours (Fig. 2g), the degraded WSF and PP were washed away by condensation water, which made these holes deeper and the whole composite became loose and porous. In Figure 3b, the matrix surrounding WSF had been hollowed out and a very deep groove on the surface could be observed, indicating that the internal structure of WS/RPP-WB had been destroyed. Therefore, the stress cannot be transferred effectively from fiber to plastic matrix and it could be the reason that WS/PP-WB showed much lower impact strength than WS/RPP-DB.

Color change

As can be seen in Figure 4 the curves of ΔL^* substantially kept in step with ΔE, indicating parameters of a^* and b^* values had a low effect on the total color change. When the weathering test began, WS/RPP-DB and WS/RPP-WB were photobleached rapidly, then slightly slowed up to 480 hours. This phenomenon could be attributed to the loss of methoxyl content of lignin in WSF, photodissociation of carbon–carbon bonds, and formation of carbonyl-based chromphoric groups (Michel and Billington 2012, Peng et al. 2014). Lignin accounted for 80 to 95 percent of light absorption, which was suggested to have made a significant effect on the discoloration (Homkhiew et al. 2014). It should be noted that the discoloration process of WS/RPP-WB was weaker than that of WS/RPP-DB, which might be because of the residual light stabilizer in PP woven bags. Usually, to prevent the performance decline of PP woven bags in the process of long-term outdoor use, some UV stabilizers are added by manufacturers (Karian 2003), which could enhance the light resistance of WS/RPP-WB to some extent. The changes in ΔE values were found to increase quickly again until 960 hours. The ΔL^* of WS/RPP-DB and WS/RPP-WB increased up to 960 hours, which were, respectively, 1.7 and 2.2 times the 240 hours. Besides the effect of UV light, the presence of condensation water enhanced the rate of photodegradation of the composites. Absorption of condensation water initiated the cell wall

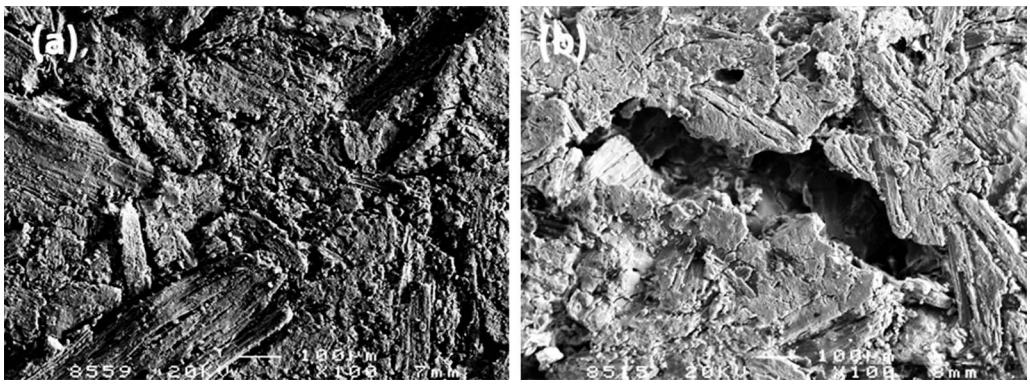

Figure 3.—Scanning electron microscope images of the wheat straw (WS)/recycled polypropylene (RPP)–disposable packaging bags (a) and WS/RPP–woven bags (b) after 1,200 hours of weathering (×200).

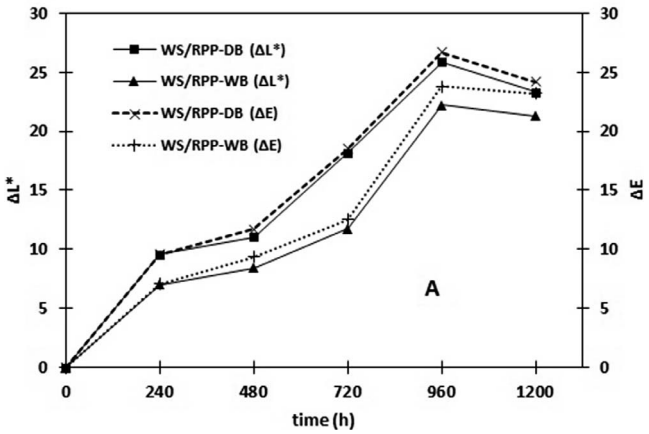

Figure 4.—Color change of wheat straw (WS)/recycled polypropylene (RPP)–disposable packaging bags and WS/RPP–woven bags after weathering.

swell of WSF to create microcracks in the matrix and facilitate UV light farther into WS/RPP (Athijayamani et al. 2009, Assarar et al. 2011). Also during the condensation process, the loose WSF particles, degraded lignin, and hemicellulose at the surface were washed away by water, which was in line with the results of the TGA discussed below in ''Thermal properties.'' The main component of WS/RPP surface was cellulose, which was whitish and comparatively stable against UV radiation (Kiguchi et al. 2007). These celluloses formed a gray fibrous layer on the surface of weathered samples and increased ΔL^* (Beg and Pickering 2008). Stark and Matuana (2003) reported that whitening of WPCs during weathering originated mainly by photobleaching the wood fiber. At 1,200 hours, ΔL^* and ΔE of WS/RPP-DB and WS/RPP-WB both declined. This was related to the surface cracks of the composite gradually extending to the interior as weathering time increased, which made the inner WSF exposed to the PP matrix.

Surface chemistry

The FTIR spectra of WS/RPP-DB and WS/RPP-WB before and after weathering are shown in Figure 5. Calculated values of the carbonyl index and lignin index are shown in Figure 6. As shown in Figure 6A, the carbonyl index of WS/RPP-WB was higher than that of WS/RPP-DB before weathering, resulting from the outdoor working conditions of RPP-WB. The presence of carbonyl groups, hydroperoxide groups, and catalyst residues could be introduced during storage, which may initiate photochemical reactions (Matuana et al. 2011). At up to 480 hours of weathering, the carbonyl index of WS/RPP-DB and WS/RPP-WB quickly increased to 8.44 and 14.5 percent, respectively, compared with that of composites before weathering, indicating that PP was photodegraded under UV exposure, resulting in the main chain scission and accretion of carbonyl products such as ketone, ester, and carboxylic acid (Rajakumar et al. 2009). Meanwhile, WSF exposed from matrix and all main polymeric components of fibers (lignin, cellulose, hemicellulose, and extractives) underwent photodegradation, in which quite a few products containing the carbonyl group were generated (Stark and Matuana 2004a, Butylina et al. 2012b). The WS/RPP-DB experienced a small drop in carbonyl index during 720 to 960 hours, which was related to the degraded WSF and PP on the surface washed away by condensation water as shown in Figure 2c. After 1,200 hours of weathering, the carbonyl index of WS/RPP-DB composite rose slightly. The increase indicated that the surface cracks of composites gradually extended to the interior, as shown in Figure 2, which initiated further photodegradation of composites. The carbonyl index of WS/RPP-WB was higher than that of WS/RPP-DB. It may relate to the impurity mingled in with RPP-WB during use, which could accelerate carbonyl group formation (Wypych 2003).

The lignin indices of WS/RPP-DB and WS/RPP-WB dropped during weathering (Fig. 6B). This probably arose from lignin photodegradation because lignin contains many UV light-absorbing groups that are very sensitive to UV light and that could form aromatic and other free radicals (Peng et al. 2014). Phenolic hydroxyl groups were changed by UV radiation rapidly to and from phenolic radicals, which transformed into quinone compounds and formation of carbonyl-based chromophoric groups (Fabiyi et al. 2008). In addition, the condensation water scoured away the WSF on the surface of the composite as shown in Figure 3, which aggravated the loss of lignin. The increase in the carbonyl index and the decrease in lignin index for WS/RPP implied that surface oxidation intensified upon weathering, and also suggested that the color change was closely related to the formation of carbonyl groups and degradation of lignin.

Thermal properties

TGA was carried out for WS/RPP-DB and WS/RPP-WB after weathering and is presented in Figure 7. The temperatures of different stages of decomposition, onset decomposition temperature (T_{onset}), temperature of maximum reaction rate (T_{max}), weight loss at T_{max} (WL_{Tmax}), and residual mass at 700°C of composites are shown in Table 1. The T_{onset} of WS/RPP-DB and WS/RPP-WB before weathering were 270.8°C and 277.8°C, respectively, compared with oriented PP and PP-WB (0 h) that were 433.9°C and 431.9°C separately, which indicated that the addition of WSF weakened the thermal stability of materials.

For WS/RPP-DB, there were three stages of weight loss: 200°C to 330°C, 330°C to 390°C, and 390°C to 500°C. The first two stages of weight loss were mainly from the thermal decomposition of WSF and the third stage was mainly from the thermal decomposition of PP matrix. The first stage of thermal decomposition was mainly attributed to hemicellulose (Alvarez and Vázquez 2004). The temperature at the first weight loss stage decreased from 307.3°C (0 h) to 303.4°C (1,200 h), which was attributed to the glycosidic bond between the monosaccharide groups being damaged by UV, and hemicellulose being degraded into small molecules, resulting in a decline of thermal stability of hemicellulose during weathering (Hosseinaei et al. 2012). It was interesting that the hemicellulose decomposition stage in WS/RPP-DB was more obvious than that in WSF (1,200 h), which was owing to the good property of WSF matrix interfacial bonding, leaving the RPP-DB matrix with better-protected WSF and reducing the external environment effect on WSF. The second weight loss stage of WS/RPP-DB was mainly caused by cellulose and lignin in WSF (Abu-Sharkh and Hamid 2004). The temperature at the second weight loss stage shifted to lower temperatures with increasing

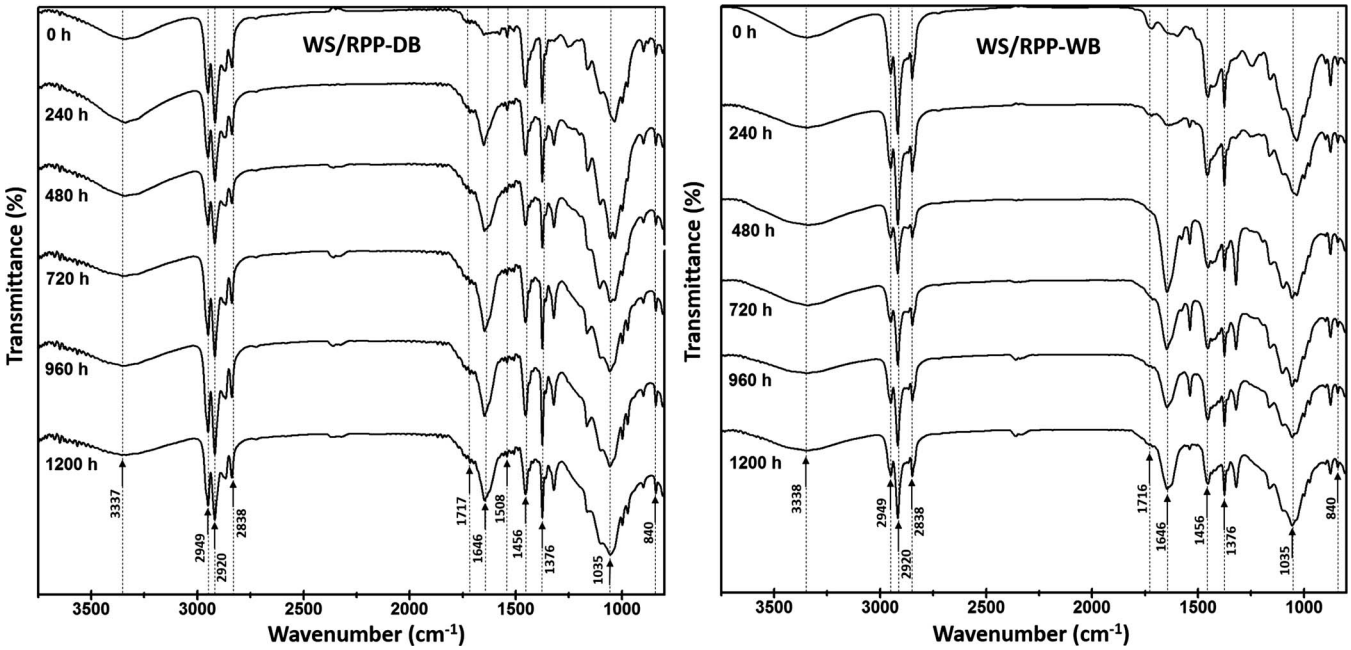

Figure 5.—Fourier transform infrared spectra of wheat straw (WS)/recycled polypropylene (RPP)–disposable packaging bags (left) and WS/RPP–woven bags (right) after weathering.

weathering time, indicating the reduction of molecular weight of cellulose and lignin because of the crystalline part of cellulose being damaged by UV radiation and the sensitive UV absorption functional groups in lignin (Peng et al. 2014). Meanwhile, many active groups like hydrogen peroxide were formed during PP degradation, which would have aggravated the photo-oxidation process of WSF, leading to decreased thermal stability (Rajakumar et al. 2009).

There were mainly two weight loss stages for WS/RPP-WB: 220°C to 380°C for WSF thermal decomposition and 390°C to 500°C for PP thermal decomposition. The hemicellulose decomposition stage in WS/RPP-WB was not as obvious as that in WS/RPP-DB, which suggested that the decomposition rate of RPP-WB was faster than that of RPP-DB; thus degraded RPP-WB could not wrap and protect WSF, leading to surface WSF exposed to UV light directly. In the thermal decomposition stage of cellulose and lignin, the T_{pk2} (peak temperature of second weight loss stage) of WS/RPP-WB shifted from 329.9°C (0 h) to 326.9°C (1,200 h), which was very close to the T_{max} of WSF after 1,200 hours of weathering (325°C). It could be inferred that RPP-WB did not wrap WSF completely, so more and more WSF were exposed to the WS/RPP-WB surface with increasing weathering time, which enhanced the surface ratio of WSF and PP matrix.

In the thermal decomposition of PP matrix, the TGA transitions for WS/RPP-DB and WS/RPP-WB both

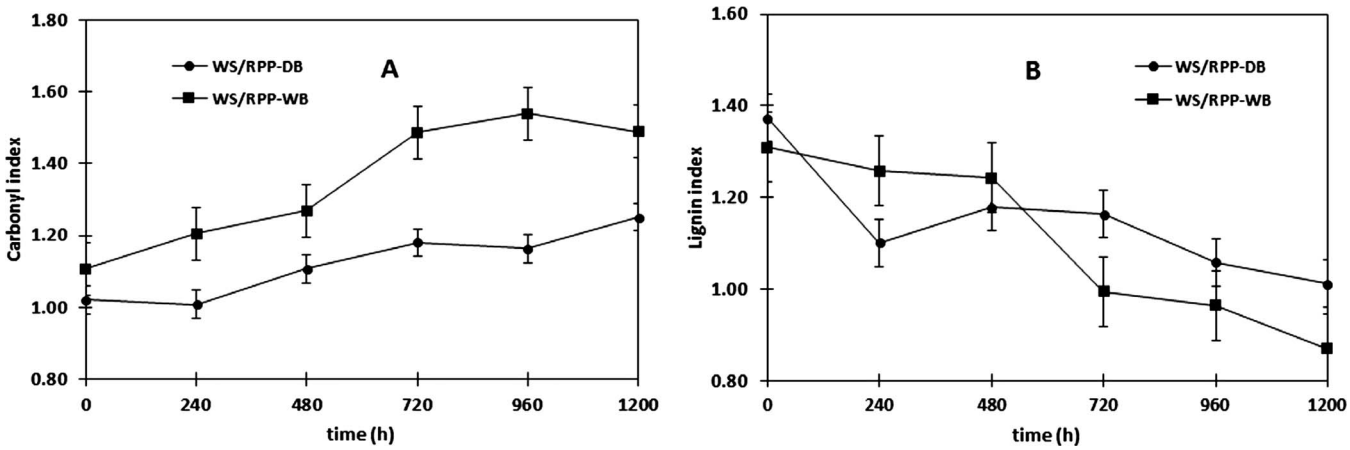

Figure 6.—Changes in the carbonyl index (A) and lignin index (B) of wheat straw (WS)/recycled polypropylene (RPP)–disposable packaging bags (DB) and woven bags (WB) after weathering.

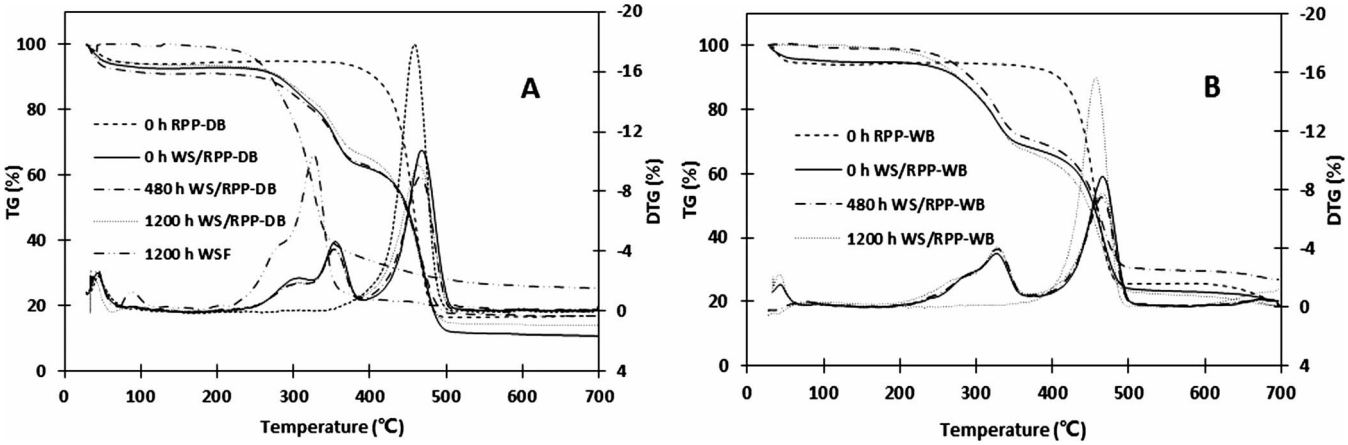

Figure 7.—Thermogravimetric analysis of wheat straw (WS)/recycled polypropylene (RPP)–disposable packaging bags (DB) (A) and WS/RPP–woven bags (WB) (B) after weathering.

shifted to lower temperatures after 1,200 hours of weathering (Table 1). The decrease in thermal stability of composites during weathering results from the PP chain scission along with degradation of both WSF and the WSF–matrix interfacial bonding (Abu-Sharkh and Hamid 2004).

Mechanical properties

The effect of accelerated weathering on flexural strength and modulus of WS/RPP-DB and WS/RPP-WB are illustrated in Figure 8. In practical applications, flexural properties were critical for the performance of WPCs (Lopez et al. 2006). It can be clearly seen in Figure 8A that flexural strength of WS/RPP-DB decreased quickly up to 720 hours, maintained steady during 720 to 960 hours, and then markedly decreased at 1,200 hours. For WS/RPP-WB, flexural strength slightly decreased up to 480 hours and then sharply decreased after 720 hours. Stark and Matuana (2003) reported that the decrease of flexural strength was related to the occurrence and development of surface cracks on composites. After 240 hours of exposure, microcracks on the WS/RPP-DB surface were already distinguishable (Fig. 2b). When they occurred from flexural forces, these cracks could cause stress concentration and reduce the efficiency of stress transfer from WSF to a plastic matrix, leading to strength decrease (Assarar et al. 2011). However, the flexural strength decrease of WS/RPP-WB was not obvious at 240 hours, which was attributed to a relatively flat surface as shown in Figure 2f. The flexural strengths of WS/RPP-DB and WS/RPP-WB deceased by 55.6 and 67.5 percent, respectively, after 1,200 hours of exposure. The trends of changes in flexural modulus of WS/RPP-DB and WS/RPP-WB were similar to the flexural strength, clearly decreasing after 240 hours. The flexural modulus of WS/RPP-DB and of WS/RPP-WB deceased by 64.9 and 64.3 percent, respectively, at 1,200 hours. The reduction in flexural modulus observed was partly a result of the negative effects of moisture penetration during exposure (Hon and Shiraishi 2000). More cracks and deep holes were observed on surfaces of WS/RPP-WB (Fig. 3b), facilitating water penetration into the internal composite, which resulted in a smaller flexural modulus than WS/RPP-DB. It was reported that the crystallinity of the composites initially increases during exposure to UV light and water, and then decreases with continued exposure (Stark and Matuana 2006). When PP is exposed to UV light, chain scissions occur. The crystalline regions are affected and crystallinity decreases when chain scission continues further (Homkhiew et al. 2014). It was expected that after 1,200 hours of exposure, the crystallinity of PP would decrease, decreasing flexural properties.

Impact strengths of WS/RPP-DB and WS/RPP-WB are illustrated in Figure 8B. After 1,200 hours of weathering, the impact strengths of WS/RPP-DB and WS/RPP-WB decreased by 22.4 and 27.4 percent, respectively. Decline in impact strength was due to poor stress transfer

Table 1.—Decomposition data of WS/RPP-DB and WS/RPP-WB.[a]

Identification	Time (h)	T_{onset} (°C)	T_{pk1} (°C)	WL_{pk1} (%)	T_{pk2} (°C)	WL_{pk2} (%)	T_{max} (°C)	WL_{Tmax} (%)	$RM_{700°C}$ (%)
WS/RPP-DB	0	270.8	307.3	2.23	356.3	5.43	469.4	11.69	10.69
	480	268.3	306.9	1.88	355	4.9	466	9.7	16.66
	1,200	268.2	303.4	1.84	347.7	4.62	464	10.54	13.76
WS/RPP-WB	0	277.8	—	—	329.9	3.98	468	9.77	20.15
	480	277.6	—	—	329.1	3.96	466.1	8.07	26.89
	1,200	274.5	—	—	326.9	4.12	464.7	7.84	18.73

[a] WS = wheat straw; RPP = recycled polypropylene; DB = disposable packaging bags; WB = woven bags; T_{onset} = onset decomposition temperature; T_{pk1} = peak temperature of the first weight loss stage; WL_{pk} = weight loss at peak temperature; T_{pk2} = peak temperature of the second weight loss stage; T_{max} = temperature of maximum reaction rate; WL_{Tmax} = weight loss at T_{max}; $RM_{700°C}$ = residual mass at 700°C.

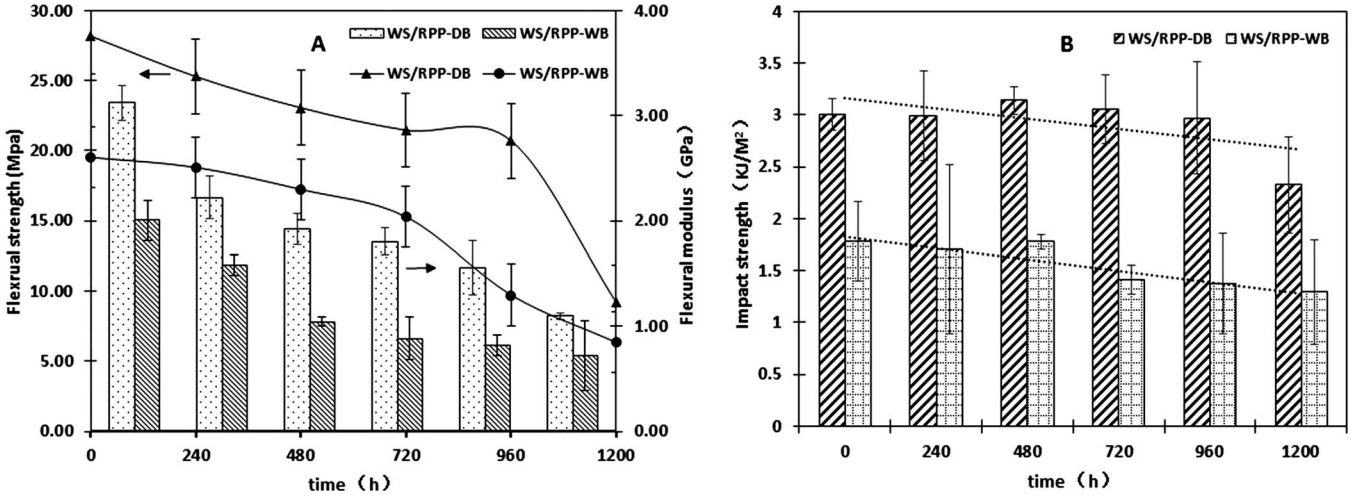

Figure 8.—Effect of accelerated weathering on mechanical properties of wheat straw (WS)/recycled polypropylene (RPP)–disposable packaging bags (DB) and WS/RPP–woven bags (WB): (A) flexural strength and (B) impact strength.

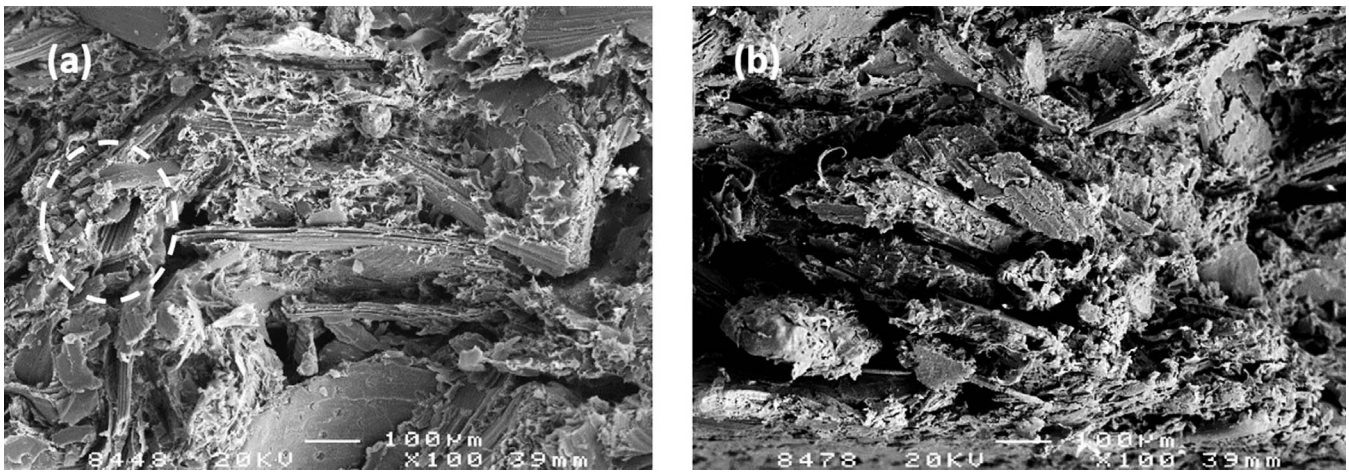

Figure 9.—Morphology of fractured surfaces of wheat straw (WS)/recycled polypropylene–disposable packaging bags (a) and WS/RPP–woven bags (b).

resulting from the degradation of the WSF–matrix interface (Stark and Matuana 2004b). The ways of energy absorption of natural fiber–reinforced composites mainly were fiber fracture, fiber pull-out, and matrix fracture. Fiber fracture could absorb the highest energy, whereas matrix fracture was the lowest (George et al. 2001). As shown in Figure 9a, a trace of WSF pull-out was observed, which suggested that the way of energy absorption of WS/RPP-DB after 1,200 hours of weathering was fiber fracture, although from the fracture surface morphology of WS/RPP-WB (Fig. 9b) the whole composite appeared to be loose and porous. As the severe degradation of RPP-WB led to poor interfacial adhesion and low efficiency of stress transfer from WSF to matrix, the main way of energy absorption of WS/RPP-WB was matrix fracture; for that reason, the impact strength of WS/RPP-WB after 1,200 hours of weathering was much lower than that of WS/RPP-DB.

Conclusions

This study used two kinds of RPP packaging bags, RPP-DB and RPP-WB with WSF as the reinforced matrix. The weathering degradation process of WS/RPP-DB was gradual from surface to interior, whereas the internal collapse aggravated the performance reduction of WS/RPP-WB. The weathering resulted in significant discoloration. The photobleaching of WS/RPP-DB was faster than that of WS/RPP-WB. The FTIR spectrum suggested that the color change was closely related to the formation of carbonyl groups and degradation of lignin. After weathering, the thermal properties of WS/RPP-DB and WS/RPP-WB were both decreased. The flexural strength and

modulus of WS/RPP strongly decreased with the exposure time. Because of the different working conditions between RPP-DB and RPP-WB, WS/RPP-DB had better performance for thermal and mechanical properties than WS/RPP-WB. RPP-DB and RPP-WB could be good candidates for utilization as matrices of WPCs for applications in the future.

Acknowledgments

The National Natural Science Foundation of China (grants 41301261 and 31300482), Natural Science Foundation of Jiangsu Province (grants BK20130680 and BK20130966), and the Doctoral Scientific Research Foundation of Shanxi University of Science & Technology (grant BJ16-01) supported this work.

Literature Cited

Abdel-Bary, E. (Ed.). 2003. Handbook of Plastic Films. Smithers Rapra Publishing, Shawbury, Shrewsbury, Shropshire, UK.

Abu-Sharkh, B. and H. Hamid. 2004. Degradation study of date palm fibre/polypropylene composites in natural and artificial weathering: mechanical and thermal analysis. *Polym. Degrad. Stab*. 85(3):967–973.

Achilias, D., E. Antonakou, C. Roupakias, P. Megalokonomos, and A. Lappas. 2008. Recycling techniques of polyolefins from plastic wastes. *Global Nest J*. 10(1):114–122.

Alvarez, V. and A. Vázquez. 2004. Thermal degradation of cellulose derivatives/starch blends and sisal fibre biocomposites. *Polym. Degrad. Stab*. 84(1):13–21.

Assarar, M., D. Scida, A. El Mahi, C. Poilâne, and R. Ayad. 2011. Influence of water ageing on mechanical properties and damage events of two reinforced composite materials: Flax–fibres and glass–fibres. *Mater. Des*. 32(2):788–795.

ASTM International. 2015. Standard practice for calculation of color tolerances and color differences from instrumentally measured color coordinates. ASTM D2244-15a. ASTM International, West Conshohocken, Pennsylvania.

Athijayamani, A., M. Thiruchitrambalam, U. Natarajan, and B. Pazhanivel. 2009. Effect of moisture absorption on the mechanical properties of randomly oriented natural fibers/polyester hybrid composite. *Mater. Sci. Eng. A* 517(1):344–353.

Azwa, Z., B. Yousif, A. Manalo, and W. Karunasena. 2013. A review on the degradability of polymeric composites based on natural fibres. *Mater. Des*. 47:424–442.

Beg, M. D. H. and K. L. Pickering. 2008. Accelerated weathering of unbleached and bleached Kraft wood fibre reinforced polypropylene composites. *Polym. Degrad. Stab*. 93(10):1939–1946.

Butylina, S., M. Hyvärinen, and T. Kärki. 2012a. Accelerated weathering of wood–polypropylene composites containing minerals. *Compos. A Appl. Sci. Manuf*. 43(11):2087–2094.

Butylina, S., M. Hyvärinen, and T. Kärki. 2012b. A study of surface changes of wood–polypropylene composites as the result of exterior weathering. *Polym. Degrad. Stab*. 97(3):337–345.

Fabiyi, J. S., A. G. McDonald, and D. McIlroy. 2009. Wood modification effects on weathering of HDPE-based wood plastic composites. *J. Polym. Environ*. 17(1):34–48.

Fabiyi, J. S., A. G. McDonald, M. P. Wolcott, and P. R. Griffiths. 2008. Wood–plastic composites weathering: Visual appearance and chemical changes. *Polym. Degrad. Stab*. 93(8):1405–1414.

George, J., M. Sreekala, and S. Thomas. 2001. A review on interface modification and characterization of natural fiber reinforced plastic composites. *Polym. Eng. Sci*. 41(9):1471–1485.

Hawkins, G. 2001. Plastic bags: Living with rubbish. *Int. J. Cult. Stud*. 4(1):5–23.

He, H. 2010. The effects of an environmental policy on consumers: Lessons from the Chinese plastic bag regulation. Environment & Development Economics 17(453).

Homkhiew, C., T. Ratanawilai, and W. Thongruang. 2014. Effects of natural weathering on the properties of recycled polypropylene composites reinforced with rubberwood flour. *Ind. Crops Prod*. 56:52–59.

Hon, D. N.-S. and N. Shiraishi. 2000. Wood and Cellulosic Chemistry, Revised, and Expanded, CRC Press, Boca Raton, Florida.

Hopewell, J., R. Dvorak, and E. Kosior. 2009. Plastics recycling: Challenges and opportunities. *Phil. Trans. R. Soc. B Biol. Sci*. 364(1526):2115–2126.

Hosseinaei, O., S. Wang, A. A. Enayati, and T. G. Rials. 2012. Effects of hemicellulose extraction on properties of wood flour and wood–plastic composites. *Compos. A Appl. Sci. Manuf*. 43(4):686–694.

Hu, R.-H., M.-y. Sun, and J.-K. Lim. 2010. Moisture absorption, tensile strength and microstructure evolution of short jute fiber/polylactide composite in hygrothermal environment. *Mater. Des*. 31(7):3167–3173.

Joseph, P., M. S. Rabello, L. Mattoso, K. Joseph, and S. Thomas. 2002. Environmental effects on the degradation behaviour of sisal fibre-reinforced polypropylene composites. *Compos. Sci. Technol*. 62(10):1357–1372.

Karian, H. 2003. Handbook of Polypropylene and Polypropylene Composites, Revised and Expanded. CRC Press, Boca Raton, Florida.

Kazemi Najafi, S. 2013. Use of recycled plastics in wood–plastic composites—A review. *Waste Manag*. 33(9):1898–1905.

Kiguchi, M., Y. Kataoka, H. Matsunaga, K. Yamamoto, and P. D. Evans. 2007. Surface deterioration of wood-flour polypropylene composites by weathering trials. *J. Wood Sci*. 53(3):234–238.

Lin, P., G. Engling, and J. Yu. 2010. Humic-like substances in fresh emissions of rice straw burning and in ambient aerosols in the Pearl River Delta Region, China. *Atmos. Chem. Phys*. 10(14):6487–6500.

Lopez, J., M. Sain, and P. Cooper. 2006. Performance of natural-fiber–plastic composites under stress for outdoor applications: Effect of moisture, temperature, and ultraviolet light exposure. *J. Appl. Polym. Sci*. 99(5):2570–2577.

Lujia, H., Y. Qiaojuan, L. Xiangyang, and H. Jinyou. 2002. Straw resources and their utilization in China. *Trans. Chin. Soc. Agric. Eng*. 3:022.

Matuana, L. M., S. Jin, and N. M. Stark. 2011. Ultraviolet weathering of HDPE/wood-flour composites coextruded with a clear HDPE cap layer. *Polym. Degrad. Stab*. 96(1):97–106.

Meran, C., O. Ozturk, and M. Yuksel. 2008. Examination of the possibility of recycling and utilizing recycled polyethylene and polypropylene. *Mater. Des*. 29(3):701–705.

Michel, A. and S. Billington. 2012. Characterization of poly-hydroxybutyrate films and hemp fiber-reinforced composites exposed to accelerated weathering. *Polym. Degrad. Stab*. 97(6):870–878.

Mukhopadhyay, S. and R. Srikanta. 2008. Effect of ageing of sisal fibres on properties of sisal–polypropylene composites. *Polym. Degrad. Stab*. 93(11):2048–2051.

Peng, Y., R. Liu, J. Cao, and Y. Chen. 2014. Effects of UV weathering on surface properties of polypropylene composites reinforced with wood flour, lignin, and cellulose. *Appl. Surf. Sci*. 317:385–392.

Rajakumar, K., V. Sarasvathy, A. T. Chelvan, R. Chitra, and C. Vijayakumar. 2009. Natural weathering studies of polypropylene. *J. Polym. Environ*. 17(3):191–202.

Reddy, C. R., A. P. Sardashti, and L. C. Simon. 2010. Preparation and characterization of polypropylene–wheat straw–clay composites. *Compos. Sci. Technol*. 70(12):1674–1680.

Standardization Administration of the People's Republic of China (SAC). 2008a. Plastic—Determination of flexural properties. GB/T 9341-2008. SAC, Beijing.

Standardization Administration of the People's Republic of China (SAC). 2008b. Plastic—Determination of charpy impact strength of rigid materials. GB/T 1043-2008. SAC, Beijing.

Stark, N. M. and L. M. Matuana. 2003. Ultraviolet weathering of photostabilized wood-flour-filled high-density polyethylene composites. *J. Appl. Polym. Sci*. 90(10):2609–2617.

Stark, N. M. and L. M. Matuana. 2004a. Surface chemistry and mechanical property changes of wood-flour/high-density-polyethylene composites after accelerated weathering. *J. Appl. Polym. Sci*. 94(6):2263–2273.

Stark, N. M. and L. M. Matuana. 2004b. Surface chemistry changes of weathered HDPE/wood-flour composites studied by XPS and FTIR spectroscopy. *Polym. Degrad. Stab*. 86(1):1–9.

Stark, N. M. and L. M. Matuana. 2006. Influence of photostabilizers on wood flour–HDPE composites exposed to xenon-arc radiation with and without water spray. *Polym. Degrad. Stab*. 91(12):3048–3056.

Winandy, J. E., N. M. Stark, and C. M. Clemons. 2004. Considerations in recycling of wood–plastic composites. *In:* Proceedings of the 5th Global Wood and Natural Fibre Composites Symposium, April 27–28, 2004, Kassel, Germany.

Wypych, G. 2003. Handbook of Material Weathering. ChemTec Publishing, Ontario, Canada.

Xing, X. 2009. Study on the ban on free plastic bags in China. *J. Sust. Dev*. 2(1):P156.

Zhang, D., Y. Shen, and G. A. Somorjai. 1997. Studies of surface structures and compositions of polyethylene and polypropylene by IR+ visible sum frequency vibrational spectroscopy. *Chem. Phys. Lett*. 281(4):394–400.

Zhang, Y., H. Dou, B. Chang, Z. Wei, W. Qiu, S. Liu, W. Liu, and S. Tao. 2008. Emission of polycyclic aromatic hydrocarbons from indoor straw burning and emission inventory updating in China. *Ann. N. Y. Acad. Sci*. 1140(1):218–227.